RESEARCH ARTICLE

Methods in Ecology and Evolution | BRITISH ECOLOGICAL SOCIETY

Mathematical and simulation methods for deriving extinction thresholds in spatial and stochastic models of interacting agents

Otso Ovaskainen[1,2] [iD] | Panu Somervuo[1] [iD] | Dmitri Finkelshtein[3] [iD]

[1]Organismal and Evolutionary Biology Research Programme, University of Helsinki, Helsinki, Finland

[2]Centre for Biodiversity Dynamics, Department of Biology, Norwegian University of Science and Technology, Trondheim, Norway

[3]Department of Mathematics, Swansea University, Swansea, UK

Correspondence
Otso Ovaskainen
Email: otso.ovaskainen@helsinki.fi

Abstract

1. In ecology, one of the most fundamental questions relates to the persistence of populations, or conversely to the probability of their extinction. Deriving extinction thresholds and characterizing other critical phenomena in spatial and stochastic models is highly challenging, with few mathematically rigorous results being available for discrete-space models such as the contact process. For continuous-space models of interacting agents, to our knowledge no analytical results are available concerning critical phenomena, even if continuous-space models can arguably be considered to be more natural descriptions of many ecological systems than lattice-based models.

2. Here we present both mathematical and simulation-based methods for deriving extinction thresholds and other critical phenomena in a broad class of agent-based models called spatiotemporal point processes. The mathematical methods are based on a perturbation expansion around the so-called mean-field model, which is obtained at the limit of large-scale interactions. The simulation methods are based on examining how the mean time to extinction scales with the domain size used in the simulation. By utilizing a constrained Gaussian process fitted to the simulated data, the critical parameter value can be identified by asking when the scaling between logarithms of the time to extinction and the domain size switches from sublinear to superlinear.

3. As a case study, we derive the extinction threshold for the spatial and stochastic logistic model. The mathematical technique yields rigorous approximation of the extinction threshold at the limit of long-ranged interactions. The asymptotic validity of the approximation is illustrated by comparing it to simulation experiments. In particular, we show that species persistence is facilitated by either short or long spatial scale of the competition kernel, whereas an intermediate scale makes the species vulnerable to extinction.

4. Both the mathematical and simulation methods developed here are of very general nature, and thus we expect them to be valuable for predicting many kinds of critical phenomena in continuous-space stochastic models of interacting agents, and thus to be of broad interest for research in theoretical ecology and evolutionary biology.

1 | INTRODUCTION

In ecology, one of the most fundamental questions relates to the persistence of populations, or conversely to the probability of their extinction. Much of our current understanding of factors influencing extinction processes comes from theoretical models. One classical example is the metapopulation model of Lande (1988) that predicted that the northern spotted owl population will go extinct if the amount of habitat destruction exceeds a threshold amount. Since the model of Lande (1988), a rich body of theory on stochastic models of population extinction has been developed (see Ovaskainen & Meerson, 2010 for a review). One particular aspect that has received much attention is how population persistence is influenced by habitat loss and fragmentation, including the spatial distribution of the remaining habitat (Fahrig, 2002). Many spatial population models are formulated in deterministic frameworks, such as reaction-diffusion models for continuous populations (Maciel & Lutscher, 2013) or systems of differential equations for metapopulations (Hanski & Ovaskainen, 2000). Spatial population models have also been formulated in stochastic frameworks, such as cellular automata models on spatial grids (Bascompte & Sole, 1996), stochastic patch occupancy models (Moilanen, 2004) or models where individuals interact in continuous space (Bolker et al., 2000; Cornell et al., 2019).

While the importance of accounting for the effects of both space and stochasticity has long been acknowledged, it is highly challenging to achieve mathematical results for spatial and stochastic population models. The separation between parameter values that determine whether the population persists or goes extinct is an example of the very broad research field of phase transitions and critical phenomena, which have been a central focus of research in theoretical physics and statistical mechanics (Domb et al., 1972–2001). As one example, the so-called contact process is a much-studied toy model of both population dynamics and the spread of infectious diseases. The contact process is a continuous-time stochastic model on a regular grid in the d-dimensional space with mesh size $1/M$ (Durrett, 1999). At any given time, each site of the grid is either vacant or occupied. Occupied sites produce propagules at rate β. The propagule lands to one of the M^d neighbouring sites, and colonizes it if it was vacant. Occupied sites go extinct at rate δ, which can be normalized to $\delta = 1$ without loss of generality. A well-known result is that there is a critical value β_c, so that if $\beta < \beta_c$, the system goes extinct, whereas if $\beta > \beta_c$, it can persist indefinitely (Durrett, 1999). However, even for the most archetypal case where the process takes place on a two-dimensional lattice, there is no exact if expression for β_c, just upper and lower bounds (Durrett, 1999). What is better understood is the mean-field limit of $M \to \infty$, at which limit the density

of occupied sites q_t at time t behaves according to the ordinary differential equation.

$$\frac{dq_t}{dt} = \beta q_t \left(1 - q_t\right) - q_t. \tag{1}$$

At this limit, it is easy to see that the critical value is $\beta_c = 1$. What is also well-understood is how β_c behaves near the mean-field limit. Namely, the difference $\beta_c(M) - \beta_c(\infty)$ between the critical value of the spatial model and its mean-field limit behaves for large M as $C \log(M)/M^2$ in the case of the two-dimensional lattice and as C/M^d in the case of d-dimensional lattice with $d \geq 3$ (Bramson et al., 1989; Durrett, 1999), where the constants C can be computed exactly (Durrett & Perkins, 1999). The single-species model of the contact process can be extended to multiple species, and the same modelling framework can be used to a rich variety of other kinds of ecologically and evolutionary relevant models (Durrett, 1999).

In this paper, we focus on a broad class of stochastic and spatial models called spatiotemporal point processes, defined in continuous space rather than the discrete-space models discussed above. While spatiotemporal point processes can be used to model a rich array of ecological and evolutionary behaviours (e.g. Barraquand & Murrell, 2013; Bolker & Pacala, 1997; Cornell et al., 2019; Murrell & Law, 2003), and while they can arguably be considered to be more natural descriptions of many ecological systems that lattice-based modes, to our knowledge there are no rigorous results concerning their critical behaviour. The analysis of spatiotemporal point processes has been mostly based on moment closure techniques (e.g. Barraquand & Murrell, 2013; Bolker & Pacala, 1997; Bolker et al., 2000; Law et al., 2003), which are intuitive but uncontrolled approximations that are not guaranteed to perform well in any particular limit (Murrell et al., 2004; Plank & Law, 2015). Thus, while analytical approximations related to extinction rates have been derived using moment closure techniques (e.g. Keeling, 2000), it is not clear at which part of the parameter space those approximations are accurate.

In this paper, we address the challenge of deriving extinction thresholds with a toy model that can be considered as a continuous-space analogue of the contact process: the Spatial and Stochastic Logistic Model (Bolker & Pacala, 1997; Law et al., 2003; Ovaskainen et al., 2014), henceforth, the SSLM. This model operates in continuous space and continuous time. The state of the model at any time t is a configuration γ_t of points in the d-dimensional Euclidean space $\mathbb{R}^d$, of which we will mostly focus on the two-dimensional case $d = 2$. The SSLM includes three processes, which we call density-independent death, density-dependent death and reproduction. In the first one, the rate at which density-independent death takes place is a constant m. In the second one, the rate of density-dependent death for an agent located at x is $\sum_{y \in \gamma_t \setminus \{x\}} a^-(x-y)$, where $a^-(x-y)$ is the
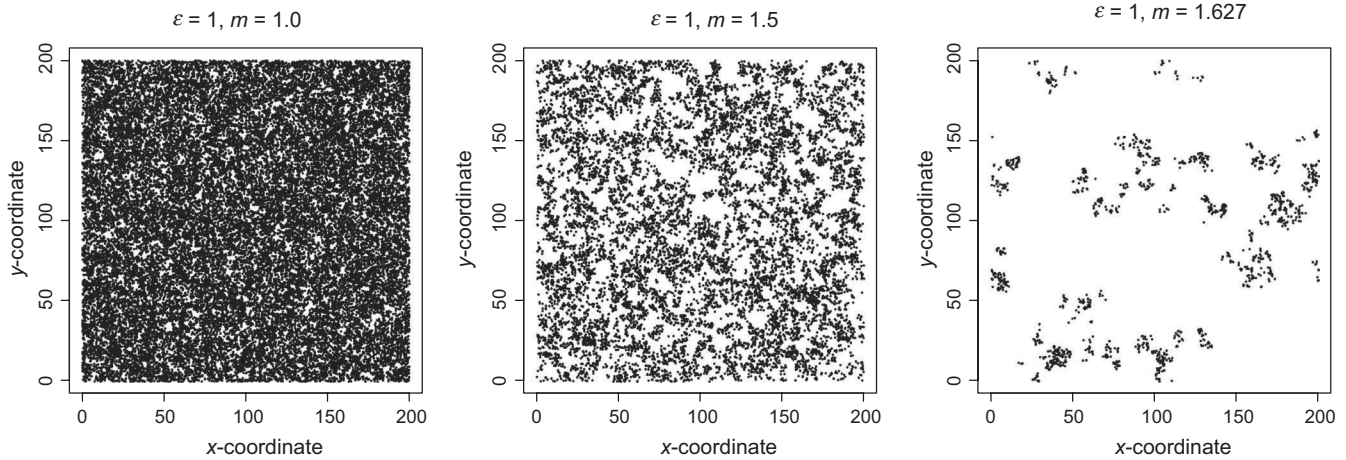
FIGURE 1 Snapshots of simulations from the quasi-stationary state of the SSLM. The dots show the locations of the individuals present at the time of the snapshot 1,000 time units after initialization. Simulations were done in a 200-by-200 unit area with periodic boundary conditions. Initial condition for individuals was Poisson with intensity of 1, reproduction kernel a^+ and competition kernel a^- had Gaussian shape $(1/2\pi)\exp\left(-|x|^2/2\right)$ with length scale $\varepsilon = 1$, and intensities $A^+ = 2$ and $A^- = 1$. For computational reasons, the Gaussians were truncated with the radius of 3. Density-independent death rate m was 1, 1.5 and 1.627 in panels from left to right, respectively

competition kernel describing the increase in death rate of an agent located at x due to the presence of another agent located at y. In the third one, the per-unit-area rate of reproduction at a location y is $\sum_{x\in\gamma_t} a^+(x-y)$, where $a^+(x-y)$ is the reproduction kernel with mother located at x and the offspring emerging to location y.

The parameters of density-dependent death and reproduction are kernels, and thus they describe both the intensity of the interaction as well as its spatial distribution. The intensity is measured by the integral of the kernel, and we denote it by $A^- = \int_{\mathbb{R}^d} a^-(x)\,dx$ for the kernel of density-dependent death, and by $A^+ = \int_{\mathbb{R}^d} a^+(x)\,dx$ for the kernel of reproduction. The spatial distribution of the kernel is further described by its shape and scale. Out of these, our special interest is in the scale parameter. To be able to vary the scale while keeping the intensity and shape constant, we introduced the scalings.

$$a_\varepsilon^-(x):=\varepsilon^d a^-(\varepsilon x), \quad a_\varepsilon^+(x):=\varepsilon^d a^+(\varepsilon x). \qquad (2)$$

These scalings preserve the integrals A^- and A^+ of the kernels but make the spatial interactions increasingly long ranged when ε approaches zero. In particular, at the limit $\varepsilon \to 0$, the model convergences to the so-called mean-field model, in an analogous way of the contact process doing so when the neighbourhood size $M \to \infty$. In the space-homogeneous case, where the population density does not depend on the space variable, the mean-field model of the SSLM is the usual logistic model of population growth, defined by the differential equation.

$$\frac{dq_t}{dt} = \left(A^+ - m\right) q_t - A^- q_t^2, \qquad (3)$$

where q_t is population density at time t. We note that Equation 3 is identical to Equation 1 up to parameterization. This mean-field model predicts that the population will go extinct if the rate of density-independent mortality is greater than the intensity of reproduction, that is if $m > A^+$, whereas the population will persist for indefinitely long time if $m < A^+$. Thus, in the mean-field model the critical value m_c (the threshold value) of the parameter m is $m_c = A^+$.

In the simulation snapshots of the stationary state of the model with local interactions ($\varepsilon > 0$), shown in Figure 1, all the other parameters of the model were kept fixed, but the rate of density-independent death m was altered. The values of the parameter m have been chosen so that the system is either much ($m = 1$), somewhat ($m = 1.5$) or just barely ($m = 1.627$) above the extinction threshold. In addition to the population density decreasing with increasing mortality, also the spatial pattern of the distribution of individuals changes. In particular, near the extinction threshold the population becomes increasingly aggregated, so that the remaining individuals form distinct patches (Figure 1). The spatial aggregation of individuals is the reason why the population goes extinct with a lower value of the mortality parameter than would be case in the mean-field model, where the critical value would be $m = 2$ in the parameterization used in our simulation. As noted by Law et al. (2003), the aggregated pattern results in elevated competition among the individuals, leading to a lower population density than in the mean-field model.

The specific research question of this paper is to find the critical value m_c of the parameter m that determines whether the population goes extinct or not, when keeping the other parameters of the model constant. This question is motivated with the much more general question of how to analyse phase transitions mathematically in spatiotemporal models. We will build our work on recent mathematical results for predicting the dynamics of a general class of models (of which the SSLM is a special case) near the mean-field limit, that is for a positive but small values of the spatial scale parameter ε. We thus seek for an expression for the critical value m_c as a function of the spatial scale parameter ε, that is an expression

for $m_c(\varepsilon)$. Based on the mean-field results, it is known that at the limit $\varepsilon \to 0$ it holds that $m_c(0) = A^+$. For small but positive ε, it is reasonable to expect that $m_c(\varepsilon)$ is close to $m_c(0)$. Our specific aim is to derive an expression for the deviation $d_c(\varepsilon) := m_c(0) - m_c(\varepsilon)$ for small ε. This deviation will describe how localized interactions influence the location of extinction threshold, compared to the case of global interactions.

2 | MATERIALS AND METHODS

2.1 | Mathematical methods

We denote by $k_{\varepsilon,t}(x)$ the expected population density at location x at time t, in a model where the kernels have been scaled with the parameter ε as in Equation 2. We consider here the translationally invariant case with homogeneous initial condition, in which case the expected population density is independent of the spatial location, and we may thus simply denote it by $u \propto \log_{10} U$. Previous work (Ovaskainen et al., 2014) has shown that, for small ε, the expected population density behaves as

$$k_{\varepsilon,t} = q_t + \varepsilon^d p_t + o\left(\varepsilon^d\right). \tag{4}$$

Here q_t is the mean-field term discussed above, p_t is the first-order correction to it and $o\left(\varepsilon^d\right)$ denotes a term that, when divided by ε^d, vanishes when $\varepsilon \to 0$. This perturbation expansion follows from a mathematically rigorous derivation (Ovaskainen et al., 2014) that is not specific to the SSLM but holds for the very general class of so-called reactant-catalyst-product models (Cornell et al., 2019), called henceforth the RCP models. We note that both the moment closure methods (see Section 1) and the perturbation expansion are approximations aimed at making the infinite hierarchy of spatial moments tractable. The main difference between these two methods is that the perturbation expansion is a mathematically controlled approximation, as it can be proved to become increasingly accurate at the limit of $\varepsilon \to 0$.

We focus on the stationary state of the model, achieved at the limit of $t \to \infty$, and denote the stationary population density by $k_\varepsilon^* = \lim_{t \to \infty} k_{\varepsilon,t}$. We further denote by $q^* = \lim_{t \to \infty} q_t$ and by $p^* = \lim_{t \to \infty} p_t$, for which the following expressions can be obtained for $A^+ > m$ (see Supporting Information):

$$q^* = \frac{A^+ - m}{A^-}, \tag{5}$$

$$p^* = -\frac{1}{A^-} \int_{\mathbb{R}^d} \frac{\tilde{a}^+(k) - q^* \tilde{a}^-(k)}{A^+ - \left(\%\tilde{a}^+(k) - q^* \%\tilde{a}^-(k)\right)} \tilde{a}^-(k) \, dk, \tag{6}$$

where $\tilde{a}$ denotes the Fourier tranform of the kernel a. In the Supporting Information, we develop a mathematical technique for deriving the leading behaviour (as $\varepsilon \to 0$) of the critical value $m_c(\varepsilon)$ that determines whether $k_\varepsilon^* > 0$. As a starting point of these derivations, we use the equation $q^* + \varepsilon^d p^* + o\left(\varepsilon^d\right) = 0$.

2.2 | Simulation methods

We used the general simulator for RCP models (Cornell et al., 2019) to determine the behaviour of $m_c(\varepsilon)$ numerically for small ε. Determining the behaviour of $m_c(\varepsilon)$ from simulations is challenging for three reasons. The first reason for this is that while the theoretical results concern the infinitely large spatial domain $\mathbb{R}^d$, simulations need to be conducted on a finite domain. We used a rectangular domain with periodic boundary conditions, and denote the size of the domain by $U \times U$. For any finite U, however large, the system goes eventually extinct with probability 1, even if the expected time to extinction can be astronomically large for cases that are much above the extinction threshold. To see why this is the case, we note that the probability of extinction is necessarily at least as great as the probability by which all individuals die before any new ones are born, which probability is positive (even if very small) for a finite system. For this reason, while in a simulation the system may appear to have reached a stationary state, mathematically it has reached only a quasi-stationary state (Darroch & Seneta, 1967). The second reason why it is difficult to determine $m_c(\varepsilon)$ from simulations is that the transient period since the initial state until reaching the quasi-stationary state can be expected to be especially long near the extinction threshold (Hanski & Ovaskainen, 2002), which is exactly the parameter regime that we are here interested about. The third reason why it is difficult to determine $m_c(\varepsilon)$ from simulations is that we are interested in the behaviour of $m_c(\varepsilon)$ for small ε, and in particular in evaluating the difference $d_c(\varepsilon)$ for small ε. With small ε, the difference $d_c(\varepsilon)$ will be small, and hence the simulations need to be the more accurate the smaller is ε.

In our simulation experiments, we fixed all the parameters of the model to those described in Figure 1, except for the focal parameter m and for the length-scale parameter ε. To mimic an infinite domain in which the system can be expected to persist indefinitely (assuming that parameter values are above the extinction threshold and that the initial condition is constant positive density), we run the simulations for increasing values of the domain size U, set as $U = 25, 50, 100, 200, 400, 800$ for the spatial models ($\varepsilon > 0$), in addition to which we applied also $U = 1600$ for the non-spatial model ($\varepsilon = 0$). To examine the behaviour of $m_c(\varepsilon)$ as a function of ε at the regime of $\varepsilon \to 0$, we varied the length-scale parameter as $\varepsilon = 1, \frac{1}{2}, \frac{1}{4}, \frac{1}{8}, \frac{1}{16}$ and $\varepsilon = 0$.

For each value of ε, we performed the simulations for a set of values of m. The selection of these was based on the mathematical results of Sagitov and Shaimerdenova (2013) on the non-spatial stochastic logistic model, thus corresponding to our case of $\varepsilon = 0$. Denoting by MTE the mean time to extinction, Sagitov and Shaimerdenova (2013) showed that the $\log$(MTE) increases linearly with $\log(U)$ for the critical value of $m = m_c$, whereas $\log$(MTE) increases sublinearly with $\log(U)$ for $m > m_c$ and superlinearly with $\log(U)$ for $m < m_c$. This behaviour is illustrated in Figure 2, where we have simulated the model with different domain sizes, for values of the parameter m that are both just below and just above the critical value of $m_c = A^+$. While we are not aware of a mathematically rigorous result that would show that the dependency of $\log$(MTE) on
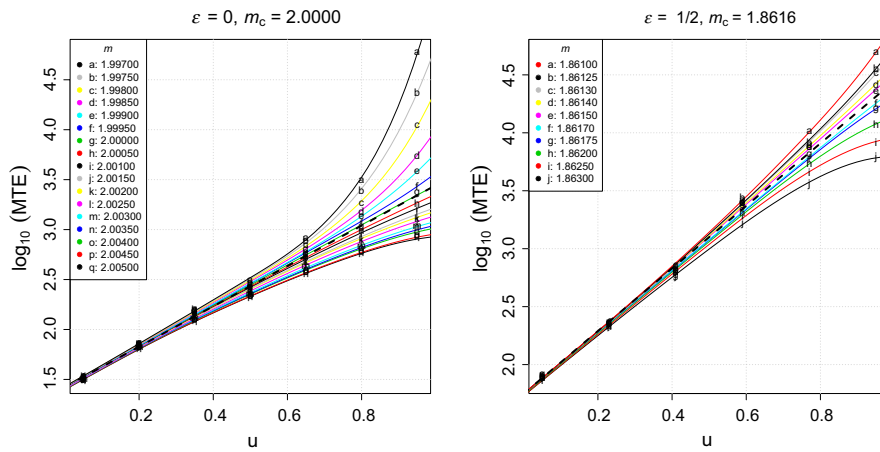
FIGURE 2 Illustration of how the critical density-independent death rate $m_c(\varepsilon)$ was estimated from simulations for each value of ε. The letters show the mean extinction time from 100 replicate simulations for each combination of density-independent death rate m and domain size $u \propto \log_{10} U$. The lines show the posterior mean prediction of a fitted constrained Gaussian process model, as explained in the Methods and in more detail in the Supporting Information. The critical density-independent death rate $m_c(\varepsilon)$ was estimated as the value m for which the Gaussian process model predicted the second derivative of the visualized curves to switch from negative to positive, as illustrated by the dashed lines, and giving the estimates shown in the tops of the panels. The parameter values of the model are set as in Figure 1. The panels show the results for the non-spatial model ($\varepsilon = 0$) and for the spatial model with $\varepsilon = 1/2$, for corresponding figures for other values of ε see the Supporting Information

$\log(U)$ would change from sublinear to superlinear at the extinction threshold also for spatial models, it is reasonable to assume that this would be the case. We thus selected a set of value of m for each value of ε so that the resulting numerically observed dependencies between $\log(\text{MTE})$ and $\log(U)$ included a switch from sublinear to superlinear behaviour. We initialized each simulation by a homogeneous Poisson process at density of 1, and continued the simulation until either the system went extinct, or until the simulation time exceeded 10^5 time units. We then estimated the mean time to extinction (MTE) as the average time to extinction from 100 replicate simulations.

For each value of ε, the simulations described above yield estimates of MTE for a combination of the parameter values m and U. To estimate the value of $m_c(\varepsilon)$ from these simulation results, we took a statistical approach, where we considered the simulated estimates of $\log(\text{MTE})$ as the response variable, and the parameters m and $\log(U)$ as explanatory variables. As a visual inspection of the data did not suggest any simple parametric relationship between the response and explanatory variables, we modelled the data as a Gaussian process (Rasmussen & Williams, 2006). We aided the model fitting by imposing a set of constrains based on qualitative a priori expectations on the systems behaviour. First, we constrained the Gaussian process with the requirement that the response variable decreases with the parameter m. Second, based on the expected switch from superlinear to sublinear behaviour, we constrained the second derivative of $\log(\text{MTE})$ with respect to $\log(U)$ to decrease from positive to negative values as a function of the parameter m. We fitted the constrained Gaussian process with the method of Maatouk and Bay (2017), the technical details being given in the Supporting Information. We then estimated the critical value m_c from the fitted model as the value of as m for which the second derivative was predicted to switch its

sign. The above-described procedure is illustrated in Figure 2 for the non-spatial case ($\varepsilon = 0$) and for a spatial case ($\varepsilon = 1/2$). We note that the estimate of $m_c(0) \approx 2.0000$ for the non-spatial case coincides with the exact value of $m_c(0) = 2$.

3 | RESULTS

The leading term of $d_c(\varepsilon)$ for small ε behaves for $d \geq 3$ as $C\varepsilon^d$, and for $d = 2$ as $CW(\varepsilon^{-2})\varepsilon^2$, or equivalently as $2C(-\log\varepsilon)\varepsilon^2$. Here $W(x)$ is the so-called Lambert W function and the dependency of the constants C on the kernels a^+, a^- and can be explicitly determined (for the derivation, see Supporting Information).

In Figure 3, we compare simulation results (dots) with analytical results (lines) for the case of $d = 2$. In the upper panels of Figure 3, we assume Gaussian kernels with identical length scales, for which case it further holds that

$$d_c(\varepsilon) = C_1 \varepsilon^2 W\left(C_2 \varepsilon^{-2}\right) + o\left(W\left(\varepsilon^{-2}\right)\varepsilon^2\right), \tag{7}$$

where the constants C_1 and C_2 are given in the Supporting Information. We note that the constant C_2 does not influence the leading term and hence may be ignored if interested only in the leading asymptotic behaviour when $\varepsilon \to 0$. In particular, these results shows that $d_c'(0) = 0$, and thus at the left-hand side of the left-hand panel the slope of the curve is exactly zero. For large ε the simulations clearly deviate from the analytical prediction, but our main interest is on verifying that the analytically derived approximation is accurate for small ε, that is that $\lim_{\varepsilon \to 0}\left(d_c^M(\varepsilon)/d_c^S(\varepsilon)\right) = 1$, where we have distinguished the mathematical (M) and simulation-based (S) solutions by the superscripts. This criterion can be written equivalently as $\log\left(d_c^M(\varepsilon)\right) - \log\left(d_c^S(\varepsilon)\right) \to 0$ as

FIGURE 3 Comparison between mathematically predicted (the lines) and simulation-based (the dots) estimates of the critical density-independent death rate $m_c(\varepsilon)$. The mathematically predicted estimates are based on Equation 7, and the simulation-based estimates are derived for each value of ε using the procedure illustrated in Figure 2. The upper panels assume equal length-scale parameters $s^+ = s^- = 1$ for the reproduction and competition kernels. The left-hand panel shows $m_c(\varepsilon)$ versus ε, whereas the right-hand panel shows the same data as $\log_2(d_c(\varepsilon))$ versus $\log_2(\varepsilon)$. The parameter values of the model (except ε) are set as in Figure 1. The lower panels show cases where $\varepsilon = 1$, one of the two length-scale parameters is fixed to the value of 1 and the other length-scale parameter is varied in a logarithmic manner
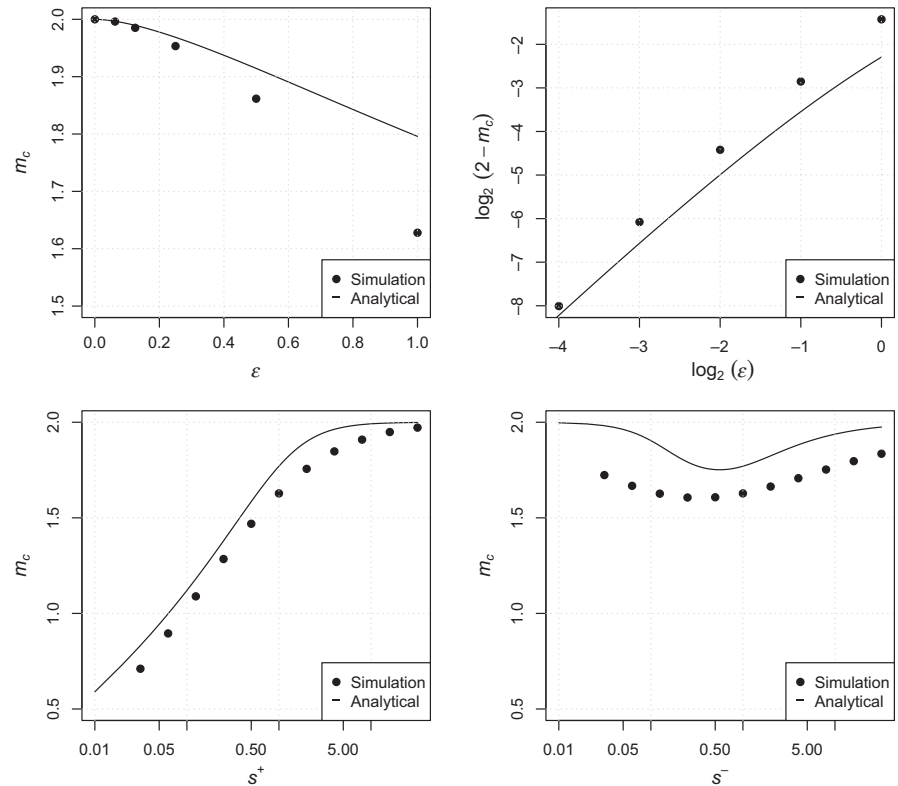
$\varepsilon \to 0$, which is indeed supported by the dots approaching the line in the upper right-hand panel of Figure 3 as $\varepsilon \to 0$.

In the lower panels of Figure 3, we have relaxed the assumption of identical length scales for the competition kernel (denoted by s^-) and the reproduction kernel (denoted by s^+). Instead, we have now fixed one of the length scales, and varied the other one in over a logarithmic scale. As the lower panels are shown for the case of $\varepsilon = 1$ rather than for the limit of $\varepsilon \to 0$, it is fully expected that the analytical predictions do not match quantitatively with the simulation results. However, the analytical and simulation results match in their qualitative behaviour. Namely, for a fixed length scale s^- of the competition kernel, the extinction threshold increases monotonically as the length scale s^+ of the reproduction kernel increases. Furthermore, for a fixed length scale s^+ of the reproduction kernel, the extinction threshold behaves non-monotonically with the length scale s^- of the competition kernel, reaching its lowest value for an intermediate value of the length scale s^-.

4 | DISCUSSION

Extinction thresholds and other critical phenomena are of central interest in theoretical ecology and evolutionary biology, but their mathematical analyses have mainly been restricted to deterministic and non-spatial models. The methods presented here greatly extend the toolbox of theoretical ecologists by enabling them to ask how extinction threshold and other critical phenomena are influenced by spatially localized interactions and stochasticity caused by the discrete nature of the interacting agents. As a case study to develop

and illustrate the methodology, we used the SSLM, which can be considered as the continuous-space analogy of the much-studied discrete-space contact process. As the parameter ε in our continuous-space model plays the role of the parameter $1/M$ in the discrete-space contact process, we note that our results are equivalent with those of the contact process (see Introduction). This is encouraging, as it suggests that the qualitative results do not depend on the technical details of how the model is implemented, for example whether space is discrete or continuous.

While we focused here on methodology rather than ecology, our results related to the length scales of reproduction and competition kernels are interesting also in terms of their ecologically interpretation. The monotonously increasing value of the extinction threshold as a function of the length scale s^+ of the reproduction kernel can be expected to be the case, because increasing the length scale of the reproduction kernel decreases the level of population aggregation, which in term decreases the adverse effect of density-dependent mortality. Perhaps less trivially, we observed that the value of the extinction threshold is minimized for an intermediate value of the length scale s^- of the competition kernel. To see why this can be expected to be the case, we note that for very large length scale of the competition kernel, the local density determining the density-dependent mortality is an average over a large spatial area, and thus the effect of density-dependent mortality is not elevated due to the local aggregation of the individuals. Conversely, for very small length scale of the competition kernel, competition is intensive but it influences only a small spatial extent. If two individuals are located close to each other, one of them will die very fast. However, with a small length scale s^-, it is rare that individuals are sufficiently close

to experience competition, and thus at the limit of $s^- \to 0$ the population-level effect of competition can be expected to vanish. The importance of spatial scales of ecological processes on the dynamics and persistence of populations has been noted also in several previous studies. For example, Murrell and Law (2003) found in a two-species model that coexistence is promoted if interspecific competition occurs over shorter distances than intraspecific competition. As another example, Keeling (2000) used moment closure methods to study how the rate of metapopulation extinction depends on what proportions of reproduction and density-dependent competition take place locally at the patch level versus globally at the metapopulation level, which proportions can be interpreted to represent spatial scales of these processes.

We developed the mathematical and simulation results specifically in the context of the SSLM (Bolker & Pacala, 1997; Law et al., 2003; Ovaskainen et al., 2014). The mathematical and simulation methods developed here are however of general nature, and thus we expect them to apply to the large class of continuous-space spatial and stochastic processes that can be formulated as RCP models (Cornell et al., 2019). In particular, as illustrated by previous studies that have applied either the RCP framework (Cornell et al., 2019) or formulated equivalent models in the terminology of spatial moment equations (e.g. Barraquand & Murrell, 2013; Murrell & Law, 2003), this family of models can incorporate any number of interacting agent types (e.g. multispecies models or models with within-species heterogeneity), as well as spatiotemporal variation in environmental conditions. The RCP methodology further applies not only to stationary state, but also to transient dynamics, as well as to inhomogeneous initial conditions (Cornell et al., 2019).

While the simulation methods presented here can be readily applied to any RCP model with arbitrary level of complexity, a limitation of the mathematical methodology is that the derivations are relatively involved (see Supporting Information), and thus it is not straightforward to systematically apply them to the general family of RCP models. In Ovaskainen et al. (2014), we developed the perturbation expansion methodology for first and second spatial moments using the SSLM as the toy model, which methods Cornell et al. (2019) later extended so that they can be easily applied to the full family of RCP models. In the same way, here we developed the extinction threshold methodology using the SSLM as a toy model, for the reason that its simplicity makes it a good test case for developing new methodology. We hope that future work will take the next step of making the methods presented here more easily applicable to the full family of RCP models. Thus, the present paper should be taken mainly as a proof of concept of it being possible to rigorously analyse extinction thresholds in continuous-space models of stochastic population dynamics.

AUTHORS' CONTRIBUTIONS

O.O. conceived the original idea and wrote the main text of the paper; P.S. performed the simulations, analysed the simulated data with constrained Gaussian process models and prepared the figures; D.F. performed the mathematical analyses and wrote the Supporting Information for them. All the authors contributed to discussions and edited the paper.

PEER REVIEW

The peer review history for this article is available at https://publons.com/publon/10.1111/2041-210X.13498.

DATA AVAILABILITY STATEMENT

This paper does not include data.

ORCID

Otso Ovaskainen https://orcid.org/0000-0001-9750-4421
Panu Somervuo https://orcid.org/0000-0003-3121-4047
Dmitri Finkelshtein https://orcid.org/0000-0001-7136-9399

REFERENCES

Barraquand, F., & Murrell, D. J. (2013). Scaling up predator-prey dynamics using spatial moment equations. *Methods in Ecology and Evolution*, *4*, 276–289. https://doi.org/10.1111/2041-210X.12014

Bascompte, J., & Sole, R. V. (1996). Habitat fragmentation and extinction thresholds in spatially explicit models. *Journal of Animal Ecology*, *65*, 465–473. https://doi.org/10.2307/5781

Bolker, B., & Pacala, S. W. (1997). Using moment equations to understand stochastically driven spatial pattern formation in ecological systems. *Theoretical Population Biology*, *52*, 179–197. https://doi.org/10.1006/tpbi.1997.1331

Bolker, B., Pacala, S. W., & Levin, S. A. (2000). Moment methods for ecological processes in continuous space. In U. Dieckmann, R. Law, & J. A. J. Metz (Eds.), *The geometry of ecological interactions: Simplifying spatial complexity* (pp. 388–411). Cambridge University Press.

Bramson, M., Durrett, R., & Swindle, G. (1989). Statistical mechanics of crabgrass. *Annals of Probability*, *17*, 444–481. https://doi.org/10.1214/aop/1176991410

Cornell, S., Suprunenko, Y., Finkelshtein, D., Somervuo, P., & Ovaskainen, O. (2019). A unified framework for analysis of individual-based models in ecology and beyond. *Nature Communications*, *10*, 4716. https://doi.org/10.1038/s41467-019-12172-y

Darroch, J. N., & Seneta, E. (1967). On quasi-stationary distributions in absorbing continuous-time finite Markov Chains. *Journal of Applied Probability*, *4*, 192–196. https://doi.org/10.2307/3212311

Domb, C., Green, M. S., Lebowitz, J. L. (Eds.). (1972–2001). *Phase transitions and critical phenomena* (Vol. 1–20). Academic Press.

Durrett, R. (1999). Stochastic spatial models. *SIAM Review*, *41*, 677–718. https://doi.org/10.1137/S0036144599354707

Durrett, R., & Perkins, E. A. (1999). Rescaled contact processes converge to super-Brownian motion in two or more dimensions. *Probability Theory and Related Fields*, *114*, 309–399. https://doi.org/10.1007/s004400050228

Fahrig, L. (2002). Effect of habitat fragmentation on the extinction threshold: A synthesis. *Ecological Applications*, *12*, 346–353.

Hanski, I., & Ovaskainen, O. (2000). The metapopulation capacity of a fragmented landscape. *Nature*, *404*, 755–758. https://doi.org/10.1038/35008063

Hanski, I., & Ovaskainen, O. (2002). Extinction debt at extinction threshold. *Conservation Biology*, *16*, 666–673. https://doi.org/10.1046/j.1523-1739.2002.00342.x

Keeling, M. J. (2000). Multiplicative moments and measures of persistence in ecology. *Journal of Theoretical Biology*, *205*, 269–281. https://doi.org/10.1006/jtbi.2000.2066

Lande, R. (1988). Demographic models of the northern spotted owl (*Strix occidentalis caurina*). *Oecologia*, *75*, 601–607. https://doi.org/10.1007/BF00776426

Law, R., Murrell, D. J., & Dieckmann, U. (2003). Population growth in space and time: Spatial logistic equations. *Ecology*, *84*, 252–262. https://doi.org/10.1890/0012-9658(2003)084[0252:PGISAT]2.0.CO;2

Maatouk, H., & Bay, X. (2017). Gaussian process emulators for computer experiments with inequality constraints. *Mathematical Geosciences*, *49*, 557–582. https://doi.org/10.1007/s11004-017-9673-2

Maciel, G. A., & Lutscher, F. (2013). How individual movement response to habitat edges affects population persistence and spatial spread. *The American Naturalist*, *182*, 42–52. https://doi.org/10.1086/670661

Moilanen, A. (2004). SPOMSIM: Software for stochastic patch occupancy models of metapopulation dynamics. *Ecological Modelling*, *179*, 533–550. https://doi.org/10.1016/j.ecolmodel.2004.04.019

Murrell, D. J., Dieckmann, U., & Law, R. (2004). On moment closures for population dynamics in continuous space. *Journal of Theoretical Biology*, *229*, 421–432. https://doi.org/10.1016/j.jtbi.2004.04.013

Murrell, D. J., & Law, R. (2003). Heteromyopia and the spatial coexistence of similar competitors. *Ecology Letters*, *6*, 48–59. https://doi.org/10.1046/j.1461-0248.2003.00397.x

Ovaskainen, O., Finkelshtein, D., Kutoviy, O., Cornell, S., Bolker, B., & Kondratiev, Y. (2014). A general mathematical framework for the analysis of spatiotemporal point processes. *Theoretical Ecology*, *7*, 101–113. https://doi.org/10.1007/s12080-013-0202-8

Ovaskainen, O., & Meerson, B. (2010). Stochastic models of population extinction. *Trends in Ecology & Evolution*, *25*, 643–652. https://doi.org/10.1016/j.tree.2010.07.009

Plank, M. J., & Law, R. (2015). Spatial point processes and moment dynamics in the life sciences: A parsimonious derivation and some extensions. *Bulletin of Mathematical Biology*, *77*, 586–613. https://doi.org/10.1007/s11538-014-0018-8

Rasmussen, C. E., & Williams, C. K. I. (2006). *Gaussian processes for machine learning*. The MIT Press.

Sagitov, S., & Shaimerdenova, A. (2013). Extinction times for a birth-death process with weak competition. *Lithuanian Mathematical Journal*, *53*, 220–234. https://doi.org/10.1007/s10986-013-9204-x

SUPPORTING INFORMATION

Additional supporting information may be found online in the Supporting Information section.